double couplings and a large excess of building blocks. The application of the A-Tag and the F-Tag to the automated synthesis of more complex oligosaccharides and other biopolymers is currently being explored.

Experimental Section

General Procedure for the automated synthesis of oligosaccharides incorporating cap-tags: Octenediol-functionalized resin **12** was loaded into a reaction vessel equipped with a cooling jacket and inserted into a modified ABI-433A peptide synthesizer. The resin was glycosylated with donor **13** or **15** (5 equiv) in CH_2Cl_2 (3 mL) with TMSOTf as activator. The suspension was mixed (10 s vortex, 50 s rest) for 15 min. The resin was then washed with CH_2Cl_2 (6×4 mL), and the unglycosylated sites were capped with A-Tag anhydride **2** or F-Tag triflate **11**. The resin was subjected to the appropriate deprotection conditions followed by the washing cycle. The deprotected polymer-bound monosaccharide was then elongated by reiteration of the above glycosylation/capping/deprotection protocol. The final trisaccharide was not deprotected, so that analysis of the products was simplified. For A-Tag, the crude material was treated with tributylphosphine and water, liberated from the resin, then purified with an isocyanate scavenger resin. For F-Tag, the crude material was liberated from the resin and purified with fluorous silica gel.

Received: August 2, 2001 [Z17654]

[1] E. Atherton, R. C. Sheppard, *Solid-Phase Peptide Synthesis: A Practical Approach*, Oxford University Press, Oxford, **1989**.

[2] M. H. Caruthers, *Science* **1985**, *230*, 281 – 285.

[3] O. J. Plante, E. R. Palmacci, P. H. Seeberger, *Science* **2001**, *291*, 1523 – 1527.

[4] a) Z. Zhang, I. R. Ollmann, X.-S. Ye, R. Wischnat, T. Baasov, C.-H. Wong, *J. Am. Chem. Soc.* **1999**, *121*, 734 – 753; b) F. Burkhart, Z. Zhang, S. Wacowich-Sgarbi, C.-H. Wong, *Angew. Chem.* **2001**, *113*, 1314 – 1317; *Angew. Chem. Int. Ed.* **2001**, 40, 1274 – 1277.

[5] S. A. Kates, F. Alberico, *Solid-Phase Synthesis: A Practical Guide*, Marcel Dekker, New York, **2000**.

[6] a) S. Funakoshi, H. Fukada, N. Fujii, *J. Chromatogr.* **1993**, *638*, 21 – 27; b) L. E. Canne, R. L. Winston, S. B. H. Kent, *Tetrahedron Lett.* **1997**, *38*, 3361 – 3364; c) M. A. Shogren-Knaak, B. Imperiali, *Tetrahedron Lett.* **1998**, *39*, 8241 – 8244; d) M. A. Shogren-Knaak, K. A. McDonnell, B. Imperiali, *Tetrahedron Lett.* **2000**, *41*, 827 – 829.

[7] a) J. R. Booth, J. C. Hodges, *Acc. Chem. Res.* **1999**, *32*, 18 – 26; b) for solution-phase tagging of carbohydrates, see V. Pozgay, *Org. Lett.* **1999**, *1*, 477 – 479; c) Y. Ito, O. Kanie, T. Ogawa, *Angew. Chem.* **1996**, *108*, 2691 – 2693; *Angew. Chem. Int. Ed. Engl.* **1996**, *35*, 2510 – 2512.

[8] a) R. Janknecht, G. de Martynoff, J. Lou, R. A. Hipskind, A. Nordheim, H. G. Stunnenberg, *Proc. Natl. Acad. Sci. USA* **1991**, *88*, 8972 – 8976; b) E. Sulkowski, *Trends Biotechnol.* **1985**, *3*, 1 – 7.

[9] S. V. Ley, A. Massi, F. Rodriguez, D. C. Horwell, R. A. Lewthwaite, M. C. Pritchard, A. M. Reid, *Angew. Chem.* **2001**, *113*, 1088 – 1090; *Angew. Chem. Int. Ed.* **2001**, *40*, 1053 – 1055.

[10] a) For a review, see D. P. Curran, *Angew. Chem.* **1998**, *110*, 1230 – 1255; *Angew. Chem. Int. Ed.* **1998**, *37*, 1174 – 1196; b) Z. Luo, Q. Zhang, Y. Oderaotoshi, D. P. Curran, *Science* **2001**, *291*, 1766 – 1769; c) D. P. Curran, Z. Luo, *J. Am. Chem. Soc.* **1999**, *121*, 9069 – 9072.

[11] C. W. Tornoe, H. Sengelow, M. Meldal, *J. Pept. Sci.* **2000**, *6*, 314 – 320.

[12] A procedure for the preparation of **11** was provided by Dr. R. Luo (Fluorous Technologies, Pittsburgh, PA).

[13] R. B. Andrade, O. J. Plante, L. G. Melean, P. H. Seeberger, *Org. Lett.* **1999**, *1*, 1811 – 1814.

From CO_2 to Methanol by Hybrid QM/MM Embedding**

Samuel A. French,* Alexey A. Sokol, Stefan T. Bromley, C. Richard A. Catlow, Stephen C. Rogers, Frank King, and Paul Sherwood

For improvements to be made in long-standing industrial catalytic processes, an understanding of the atomistic mechanisms of the reactions occurring on the surface of the catalyst is required. A variety of experimental techniques can be used to derive information on sorption and reaction processes, but when both the catalyst and reactant mixtures are multicomponent, unambiguous identification of reaction mechanisms is difficult and often controversial. Computational techniques can, however, be used to gain valuable insight and interpret experimental evidence. Herein we show how new methods for modeling surface reactions on oxides can be used to elucidate key steps in a widely studied catalytic process—the conversion of CO_2 to methanol over oxide catalysts.

A large quantity of methanol (in excess of 25 million tonnes worldwide) is produced annually using the multicomponent $Cu/ZnO/Al_2O_3$ catalyst and $CO_2/CO/H_2$ as the feed gas. Many experimental studies of this process have been performed, but no definite reaction mechanism for the production of methanol has been established. However, it has long been acknowledged that the important rate-determining step is the hydrogenation of adsorbed intermediates, for example, the formate ion, at the active sites. Proposed mechanisms for methanol synthesis require the chemisorption of CO_2 before hydrogenation via formate to methanol. Theoretical studies of these systems have been hampered by the difficulty of modeling the catalytically active polar surfaces of ZnO, as well as by problems associated with the restrictions on the size of the system that can be modeled.

The nature of the active site for sorption/catalysis of CO_2 still remains unclear; it has been proposed to use clean oxygen-terminated surfaces of zincite as a test system or model catalyst. Temperature-programmed desorption (TPD) studies have shown that the processes that occur at that

[*] Dr. S. A. French, Dr. A A. Sokol, Dr. S T. Bromley, Prof. C. R. A. Catlow
Davy Faraday Research Laboratory
The Royal Institution of Great Britain
21 Albemarle Street, London, W1S 4BS (UK)
Fax: (+44) 20-7670-2920
E-mail: sam@ri.ac.uk

Dr. S C. Rogers
ICI Strategic Technology Group
Wilton Centre, PO Box 90, Redcar, TS90 8JE (UK)

Dr. F King
Synetix, Belasis Avenue
Billingham, TS23 1LB (UK)

Dr. P Sherwood
CLRC Daresbury Laboratory
Warrington, WA4 4AD (UK)

[**] This work was supported by EU Esprit IV project 25047. S.A.F. is grateful to ICI and Synetix for funding. K. Waugh, L. Whitmore, S. Cristol, and P. Sushko are thanked for their helpful insights. QM/MM = quantum mechanics/molecular mechanics.

particular surface are analogous to those on the industrial Cu/ZnO/Al_2O_3 catalyst.[1] In this study we have therefore concentrated on the polar $(000\bar{1})$ oxygen-terminated surface. The polar character of the surface of a given sample necessitates charge transfer between opposing polar surfaces. One mechanism of quenching the surface polarization is to abstract approximately 25% of the oxygen ions from the surface layer, thus creating *vacant oxygen interstitial surface sites*. The presence of such sites has been confirmed by optical and electron spin resonance (ESR) spectroscopies.[2] They have, moreover, been suggested as the active catalytic sites for methanol synthesis and are, therefore, the focus of the investigation presented here. We have studied the adsorption of important methanol precursors including carbon dioxide, formate, and methoxy ions. We have calculated binding energies, bond lengths, and angles of these and related species to provide insight into the mechanism of methanol synthesis.

In order to pursue these studies a novel solid-state embedding technique has been developed based on a hybrid QM/MM approach by employing molecular embedded cluster methods developed to treat point defects and localized states in ionic materials.[3] At the heart of embedding approaches is a definition of a reference system and a single localized state, which causes only minor long-range perturbation of the reference system. These methods have a rigorous foundation in the many electron theories of localization and separability,[4] and are more appropriate for the present study than are related embedding methods employed in the fields of zeolites and biochemistry.[5]

All ions, but especially anions, are polarizable species. Two major effects are witnessed upon perturbation of the reference system by a localized defect: 1) dramatic short-range effects, (for example, charge transfer and bond breaking) and 2) long-range polarization of electron groups (for example, ions) as a result of the field associated with the defect. Therefore, the model can be treated at two levels of approximation. In the present work the short-range effects are dealt with by fully ab initio methods (density functional theory (DFT)), while the long-range polarization effects are included through the use of the shell model of Dick and Overhauser.[6]

Thus, our structural model is split into two major regions: region 1 being treated by ab initio methods and region 2 with pairwise interatomic potentials. The short- and long-range interactions between regions 1 and 2 require careful attention: the former is handled by an interface between regions 1 and 2, while the latter is described by a mesh of point charges fitted to reproduce the lattice Madelung field at the area of interest.[7] The interface is formed by short-range-localizing model potentials, which act on electrons. In this work such potentials have only been associated with cationic sites, while anionic sites in the interface region were represented simply by point charges and classic interatomic potentials. Relaxation resulting from the defect has been allowed up to a certain cut-off radius, which includes all of region 1 and part of region 2 (typically of the order of 600 atoms; Figure 1).

The methodology described was implemented within ChemShell, which is a computational chemistry environment, based on the Tcl programming language.[7] A DFT treatment,

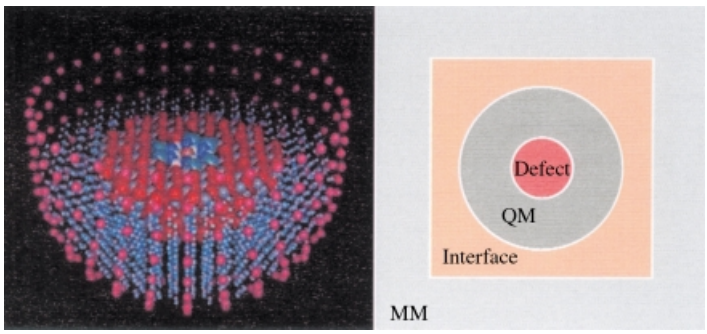

Figure 1. Embedded cluster model used in this work.

as implemented in the GAMESS-UK code, was used.[8] We employed the B97-1[9] exchange correlation functional and TZV2P basis set on O and Zn atoms, which was reoptimized for the ionic state of ZnO (details will be reported elsewhere), along with the standard 6-311 + (2p2d) basis set on all atoms of the adsorbates and a medium quality integration mesh.[8] Interactions in region 2 and at the interface were dealt with using our recently developed atomistic potentials[10] within the GULP code.[11]

Detailed models of the $(000\bar{1})$-0 terminated polar surfaces were investigated using interatomic potentials and the two-dimensional periodic slab model realized within the MARVIN code.[12] Two typical local environments were identified as terrace termination and interstitial vacancy sites; the latter has been used as the active site for the majority of calculations (Figure 2). The atoms highlighted in the figure indicate the

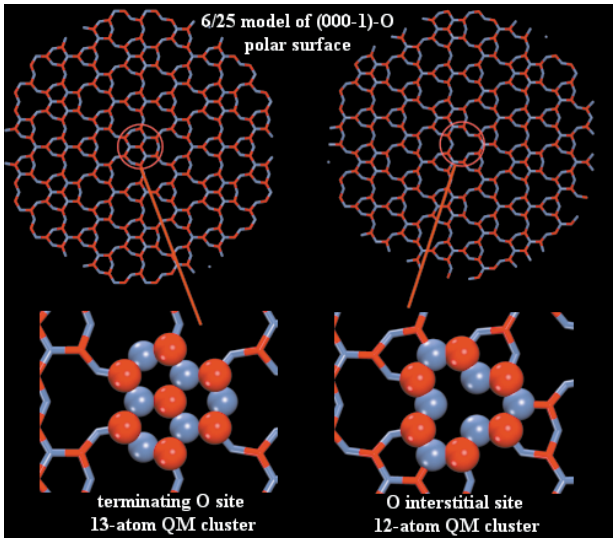

Figure 2. QM regions used for the modeling of vacant oxygen interstitial surface sites. Only the upper surface layer is shown.

surface-embedded quantum region. For the calculations reported, region 1 consists of 12 atoms, the interface has 13 Zn sites, while region 2 comprises approximately 3000 atoms and 250 terminating point charges.

We have undertaken a series of calculations on the reactants, intermediates, and products of methanol synthesis by using the embedding technique described earlier. A

  0044-8249/01/11323-4570 $ 17.50+.50/0

probable reaction sequence for the conversion of the feed gas to methanol has been summarized by Chinchen et al.:[13]

$$H_2(g) \longrightarrow 2H(a) \quad (1)$$

$$CO_2(g) \longrightarrow CO_2(a) \quad (2)$$

$$CO_2(a) + H(a) \longrightarrow HCO_2(a) \quad (3)$$

$$HCO_2(a) + 2H(a) \longrightarrow CH_3O(a) + O(a) \quad (4)$$

$$CH_3O(a) + H(a) \longrightarrow CH_3OH(g) \quad (5)$$

$$CO(g) + O(a) \longrightarrow CO_2(g) \quad (6)$$

$$H_2(g) + O(a) \longrightarrow H_2O(g) \quad (7)$$

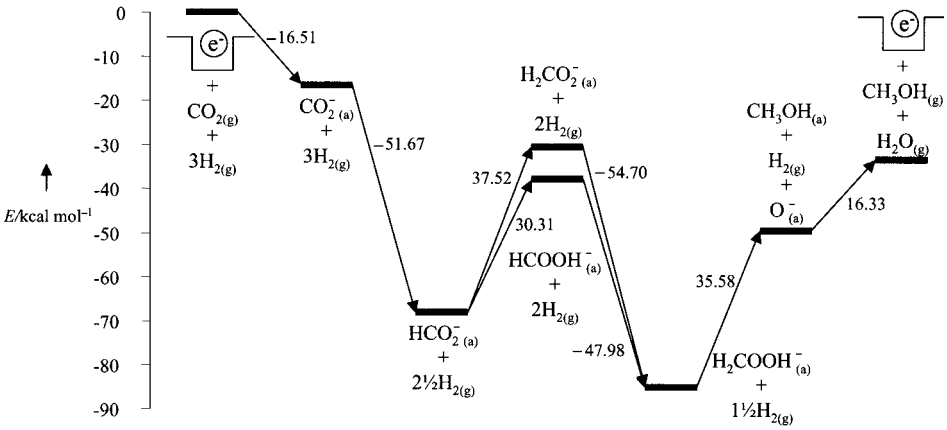

Figure 3. Calculated reaction energy profile for methanol synthesis over ZnO.

The gas-phase and adsorbate species are indicated by (g) and (a), respectively.

Reaction 4 is a complex process that includes multiple hydrogenation steps, which we have considered separately. The resulting species, which were not considered by Chinchen et al. and others, we find to be stable, although they may possibly be transient and short-lived.

The main catalytically active site that can facilitate the formation of anionic adsorbates is the oxygen interstitial site (as described above and illustrated on the right hand side of Figure 2). This site is able to trap an electron and thus adsorption can occur in two different ways: 1) neutral adsorbates approach the active site at which an electron is trapped and form an anionic surface species, and 2) the transfer of an electron to the neutral active site occurs simultaneously with the adsorption of neutral adsorbates.

The proposed catalytic cycle is summarized in Scheme 1, with the calculated energetics given in Figure 3, which is discussed in greater detail below. We start with the adsorption of CO_2 [Eq. (2)] and H_2 [Eq. (1)]. (Detailed studies of the latter will be reported elsewhere shortly.) CO_2, upon adsorption in a neutral interstitial site, retains the linear structure exhibited in the gas phase. On adding an electron the neutral CO_2 molecule bends and the extra electron populates an antibonding level, which leads to a rearrangement from an sp- to an sp^2-hybridized configuration. (The angle changes from 179.9 to 127.3°.) The interaction with the surface stabilizes the radical CO_2^- species.

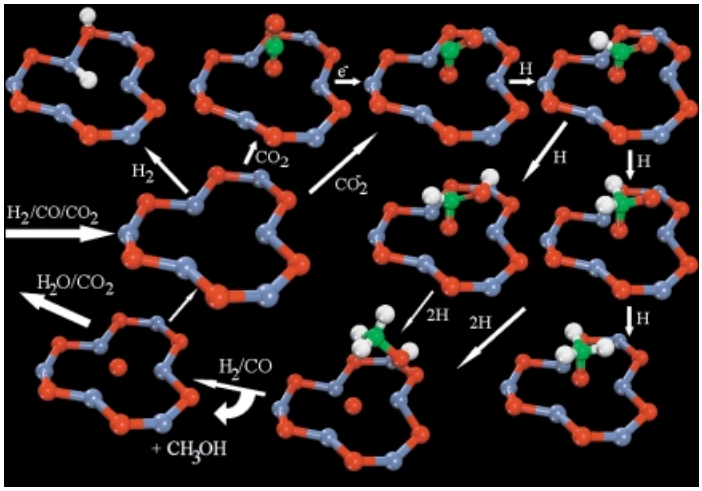

Scheme 1. Catalytic cycle: The geometries of all the reactants are obtained by energy minimization of embedded clusters.

The reaction then proceeds by the hydrogenation of the adsorbed CO_2^- species, by surface hydrogen [Eq. (1)], to the formate ion [Eq. (3)].[13] The geometry resulting from our calculations is shown in Scheme 1. The adsorption of hydrogen leads to a closed-shell species. Further hydrogenation can proceed either through the formation of $H_2CO_2^-$ or $HCOOH^-$ (formic acid) as shown in Scheme 1. Temperature-programmed desorption data do not detect these species, which suggests they have a short lifetime and, therefore, high reactivity. Computational techniques allow us to differentiate and investigate these different mechanisms. Further hydrogenation and interactions of the resulting species with the surface and possible surface defects lead to a large variety of possible intermediates. Examples of a methoxy ion [Eq. (4)] (CH_3O^-) chemisorbed onto the surface and physisorbed methanol [Eq. (5)] are also shown in Scheme 1. To complete the catalytic cycle, methanol is removed from the surface and the active site is recycled by desorption of carbon dioxide [Eq. (6)] and water [Eq. (7); Scheme 1].

The structural data are summarized in Table 1. We note that the vacant oxygen interstitial site accommodates both an electron and an oxygen (O^-) anion, thus restoring the terrace-like surface termination. We observe that there is a general trend with the adsorbates for charge transfer towards the

Table 1. Calculated structural parameters of adsorbate species at the vacant oxygen interstitial surface site.

Species	O_a–C [Å]	C–O_b [Å]	O_a-C-O_b [°]	C–H [Å]
CO_2	1.19	1.15	179.9	–
CO_2^-	1.35	1.20	128.3	–
HCO_2^-	1.33	1.23	120.4	1.09
$H_2CO_2^-$	1.43	1.35	112.5	1.11
$HCOHO^-$	1.39	1.38	112.1	1.09
H_3CO^-	1.47	–	–	1.09
H_3COH	3.45	1.44	–	1.09

  0044-8249/01/11323-4571 $ 17.50+.50/0

surface and a corresponding polarization of the chemical bonds in the adsorbate. These effects are shown both in the charge distribution and in the elongation of the lower oxygen–carbon bond relative to those in the gas-phase structures. (In contrast, the alcoholic hydrogen–oxygen bond length has a typical value of 0.97 Å in all the relevant species studied.)

We have calculated the surface adsorption energies by comparing the total energies of the embedded clusters with and without adsorbed species. These calculations are of particular interest as a comparison can be made with experiment. The desorption process considered includes desorption from a neutral and vacant oxygen interstitial site as well as from an adsorbed O^- species. However, as we have concentrated on the catalytically relevant reactants, intermediates, and products, we are only able to compare two models directly with experimental results. The complexity of the preparation of the samples and the reactions, which occur in the adsorption/desorption experimental cycle in the TPD work, prevents us, currently, from making a direct comparison, but this will be addressed in the near future by using calculations that relate directly to the desorption process.

Both experimental desorption energies have been obtained from the low-temperature adsorption of carbon dioxide as reported by Bowker et al.[1b] About 10% of the adsorbed carbon dioxide dissociates to carbon monoxide upon TPD which, therefore, heals the surface defects. We calculate the abstraction of CO_2 from the vacant oxygen interstitial surface site with a trapped electron to be 69 kJ mol^{-1}, which compares to an experimental desorption energy of 109–117 kJ mol^{-1}. The value we calculate provides a lower limit for the adsorption energies as: 1) we neglect the polarization effects beyond a certain cut-off radius (12.5 Å from the QM region), although such effects are likely to be small; and 2) the observed values refer to the free energy, and thus include vibrational contributions, which are omitted from our current study. The energy of desorption of CO is calculated as an energy of cleavage of the O_a–C bond in the CO_2^- adsorbate (as suggested by Bowker et al.) and is found to be 113 kJ mol^{-1}; this value compares favorably to the experimental value of 109 kJ mol^{-1}. The current method slightly overestimates the covalent bonding, which is common to all DFT simulations.

The adsorption energies calculated for other species shown in Scheme 1 allow us to obtain the reaction energies for the full catalytic cycle (Figure 3). The hydrogenation of adsorbates is shown to drive the reaction over the active site, in agreement with experiment. Our calculation uses half of the total energy of gas-phase H_2, thus all our energies are given with respect to molecular gaseous hydrogen as the base line. Two intermediate species are shown to be particularly stable, namely HCO_2^- and H_2COOH^-. The former (the formate ion) is known to be a stable long-lived intermediate,[1b] but the latter has not been experimentally characterized, although it is isomeric with the methoxy species which has been reported.[13]

Our methodology clearly has the ability to elucidate a detailed and quantitative mechanism for the catalytic processes involved in this important reaction. Furthermore, it can be readily extended to include other fields of surface and materials science. Moreover, this approach can be used to calculate electronic, spectroscopic, and other properties of sorbed molecules.

Received: July 23, 2001 [Z17561]

[1] a) V. E. Heinrich, P. A. Cox, *The Surface Science of Metal Oxides*, Cambridge University Press, Cambridge, **1996**; b) M. Bowker, H. Houghton, K. C. Waugh, *J. Chem. Soc. Faraday Trans. 1* **1981**, *77*, 3023; c) K. M. Vandenbusche, G. F. Froment, *App. Catal. A* **1994**, *112*, 37; d) S. Bailey, G. F. Froment, J. W. Snoeck, K. C. Waugh, *Catal. Lett.* **1995**, *30*, 99; e) I. Nakamura, H. Nakano, T. Fujitani, T. Uchijima, J. Nakamura, *Surf. Sci.* **1998**, *404*, 92; f) K. R. Harikumar, C. N. R. Rao, *Appl. Surf. Sci.* **1998**, *125*, 245.

[2] a) K. Vanheusden, C. H. Seager, W. L. Warren, D. R. Tallant, J. Caruso, M. J. Hampden-Smith, T. T. Kodas, *J. Luminescence* **1997**, *75*, 11; b) A. R. Gonzalez-Elipe, J. Soria, *J. Chem. Soc. Faraday Trans. 1* **1988**, *84*, 3961; c) B. Yu, C. Zhu, F. Gan, Y. Huang, *Mater. Lett.* **1998**, *33*, 247.

[3] a) J. H. Harding, A. H. Harker, P. B. Keegstra, R. Pandey, J. M. Vail, C. Woodward, *Physica B* **1985**, *131*, 151; b) A. L. Shluger, E. A. Kotomin, L. N. Kantorovich, *J. Phys. C* **1986**, *19*, 4183; c) Z. Barandiarán, L. Seijo, *J. Chem. Phys.* **1988**, *89*, 5739; d) M. N. Nygren, L. G. M. Petersson, Z. Barandiaran, L. Seijo, *J. Chem. Phys.* **1994**, *100*, 2010; e) P. V. Sushko, A. L. Shluger, C. R. A. Catlow, *Surf. Sci.* **2000**, *450*, 153.

[4] a) S. Huzinaga, A. A. Cantu, *J. Chem. Phys.* **1971**, *55*, 5543; b) R. McWeeny, *Methods of Molecular Quantum Mechanics*, 2nd ed., Academic Press, London, **1992**; c) L. N. Kantorovich, *Int. J. Quantum Chem.* **2000**, *78*, 306.

[5] a) U. Eichler, C. M. Kolmel, J. Sauer, *J. Comp. Chem.* **1996**, *18*, 463; b) M. Sierka, J. Sauer, *Faraday Discuss.* **1997**, *106*, 41; c) J. Gao, *Acc. Chem. Rev.* **1996**, *29*, 298; d) I. Antes, W. Thiel, *J. Phys. Chem. A* **1999**, *103*, 9290.

[6] B. G. Dick, A. Overhauser, *Phys. Rev.* **1958**, *112*, 90.

[7] P. Sherwood, A. H. Devries, S. J. Collins, S. P. Greatbanks, N. A. Burton, M. A. Vincent, I. H. Hillier, *Faraday Discuss.* **1997**, *106*, 79.

[8] GAMESS-UK is a package of ab initio programs written by M. F. Guest, J. H. van Lenthe, J. Kendrick, K. Schoffel, and P. Sherwood, with contributions from R. D. Amos, R. J. Buenker, H. J. J. van Dam, M. Dupuis, N. C. Handy, I. H. Hillier, P. J. Knowles, V. Bonacic-Koutecky, W. von Niessen, R. J. Harrison, A. P. Rendell, V. R. Saunders, A. J. Stone, D. J. Tozer, and A. H. de Vries. The package is derived from the original GAMESS code: M. Dupuis, D. Spangler, J. Wendoloski, *NRCC Software Catalog*, *Vol. 1*, Program No. QG01 (GAMESS), **1980**.

[9] F. H. Hamprecht, A. J. Cohen, D. J. Tozer, N. C. Handy, *J. Chem. Phys.* **1998**, *109*, 6264.

[10] L. Whitmore, A. A. Sokol, C. R. A. Catlow, *Surf Sci.* **2001**, in press.

[11] J. D. Gale, *J. Chem. Soc. Faraday Trans.* **1997**, *93*, 629.

[12] D. H. Gay, A. L. Rohl, *J. Chem. Soc. Faraday Trans.* **1995**, *91*, 92.

[13] G. C. Chinchen, M. S. Spencer, K. C. Waugh, D. A. Whan, *J. Chem. Soc. Faraday Trans. 1* **1987**, *83*, 2193.

  0044-8249/01/11323-4572 $ 17.50+.50/0